measurements[14] carried out on samples of the $[Pt_9(CO)_{18}]^{2-}$, $[Pt_{24}(CO)_{30}]^{2-}$, $[Pt_{26}(CO)_{32}]^{2-}$, and $[Pt_{38}(CO)_{44}]^{2-}$ dianions and the $[Pt_{19}(CO)_{22}]^{4-}$ tetraanion.[15,16] Both positive- and negative-ion mass spectra of these cluster anions are of interest in that (1) they emphasize that ^{252}Cf-PDMS is an excellent tool to probe platinum stoichiometry of high-nuclearity platinum carbonyl anions because the parent ion platinum core peak is the strongest signal observed in each sample, and (2) they all display high-mass ion peaks corresponding to oligomers of the parent ion platinum core fragment in each anion.

Figure 1 presents a positive-ion mass spectrum of the $[PPh_3Me]^+$ salt of the $[Pt_{26}(CO)_{32}]^{2-}$ dianion which contains a three-layer (7:12:7) hcp Pt_{26} core of pseudo-D_{3h} symmetry.[15,17] This positive-ion mass spectrum exhibits an extraordinary series of high-mass, monocharged $[Pt_{26}(CO)_x]_n^+$ peaks which extend from m/z 5746 for the major Pt_{26} core peak ($n = 1$) to m/z 107 045 for the Pt_{520} core peak ($n = 20$). This latter peak corresponds to the highest m/z ion to be detected by ^{252}Cf-PDMS. Each of these high-mass peaks consists of a complex envelope due not only to the different number (x) of carbonyl ligands attached to the platinum core for a given value of n but also to the various isotopic combinations[18] for a given molecular formula. Thus, the envelope of the major parent ion peak ranges from the fully decarbonylated species at the low-mass limit to the fully carbonylated cluster at the high-mass limit with the peak centroid most nearly conforming to the $[Pt_{26}(CO)_{24}]^+$ ion (5744 u). A similar pattern of monocharged parent ion and oligomer ion peaks is observed in the negative-ion spectrum as well. The extent of self-condensation of the Pt_{26} core is most remarkable and indicates strong cluster aggregation.

^{252}Cf-PDMS of different salts of the other platinum carbonyl anions also provided highly desirable information. It is particularly noteworthy that mass spectra of the $[Pt_{24}(CO)_{30}]^{2-}$ and $[Pt_{38}(CO)_{44}]^{2-}$ dianions also exhibited high-mass peaks corresponding to oligomerization of their parent ion ccp platinum cores. In contrast, mass spectra of the $[Pt_9(CO)_{18}]^{2-}$ dianion and $[Pt_{19}(CO)_{22}]^{4-}$ tetraanion displayed high-mass peaks involving only a small amount of dimerization ($n = 2$) of their non closest packed platinum cores. Mass spectra of the former complex also contained peaks due to the addition of Pt_3 units.

The negative-ion spectrum of the $[(Ph_3PCH_2C_5H_4)Fe(C_5H_5)]^+$ salt of the $[Pt_9(CO)_{18}]^{2-}$ dianion, whose idealized D_{3h} symmetry involves an eclipsed superposition of three $Pt_3(CO)_3(\mu_2\text{-}CO)_3$ building blocks, contained an intense parent ion envelope corresponding to $[Pt_9(CO)_x]^-$ with clearly resolvable peaks differing by carbonyl units varying from $x = 4$ to $x = 16$ with the principal peak centered at $x = 8$. Of prime interest was the occurrence of a multiplet set of monoanion peaks for Pt_{12}, Pt_{15}, Pt_{18}, and Pt_{21} cores. A slightly more intense peak envelope was observed for the dimeric $[Pt_{18}(CO)_x]^-$ multiplet ($n = 2$) than for the $[Pt_{12}(CO)_x]^-$ and $[Pt_{15}(CO)_x]^-$ multiplets. The fact that a spectroscopic (near-IR/near-UV) analysis[19] revealed that controlled oxidation of the $[Pt_9(CO)_{18}]^{2-}$ dianion in THF solution with the $[FeCp_2]^+$ cation gave not only the Chini–Longoni $[Pt_{12}(CO)_{24}]^{2-}$, $[Pt_{15}(CO)_{30}]^{2-}$, and $[Pt_{18}(CO)_{36}]^{2-}$ dianions[12,13] but also the previously unknown $[Pt_{21}(CO)_{42}]^{2-}$ and $[Pt_{24}(CO)_{48}]^{2-}$ dianions is consistent with these gas-phase species likewise being composed of trigonal-prismatic stacks of platinum triangles.

This work illustrates the general applicability of ^{252}Cf-PDMS for analyzing a wide variety of high-nuclearity anionic metal clusters. Furthermore, it represents a new evolution in the application of the high-mass capabilities of ^{252}Cf-PDMS, which has heretofore been limited to compounds of biological interest. Further work in progress includes studies of the effects of sample dilution on the formation of gas-phase oligomer ions from the solid-state $[Pt_{26}(CO)_{32}]^{2-}$ dianions and the determination of the fragmentation patterns for other triangular $[Pt_3(CO)_6]_n^{2-}$ dianions.

Acknowledgment. We are especially grateful to Professor Ron Macfarlane for the use of the ^{252}Cf-PD mass spectrometer. This research was supported by the National Science Foundation (Grants CHE-8616697 and CHE-9013059), the Robert A. Welch Foundation (Grant A-258), and the National Institutes of Health (Grant GM26096), the latter two awarded to R. D. Macfarlane. J.M.H. was supported by a Minority Merit Fellowship from the Office of Graduate Studies (Texas A&M University). G.J.L. acknowledges Mr. Arthur J. Kahaian for his assistance in the synthetic phases of this work. We thank Mr. Randy K. Hayashi for his assistance in the preparation of this manuscript. We are most pleased to acknowledge the Johnson-Matthey Inc. loan program (West Deptford, NJ) for supplying a sample of chloroplatinic acid, from which the platinum carbonyl clusters were prepared.

---

(14) ^{252}Cf-PDMS was performed on solid samples that had been electrosprayed as ca. 10^{-3} M solutions onto a thin Au/Al-coated Mylar polyester film. The samples were initially weighed inside a Vacuum Atmospheres glovebox and then transferred to a N_2-purged glovebag enclosing the inlet probe, where they were dissolved in either THF or acetonitrile. A detailed description of the time-of-flight instrument (locally designed and constructed) with the ^{252}Cf-plasma desorption ionization probe and the data acquisition system is given elsewhere.[3]

(15) Descriptions and figures of the platinum core geometries of these clusters are given elsewhere.[16]

(16) Kharas, K. C. C.; Dahl, L. F. *Advances in Chemical Physics*; Prigogine, I., Rice, S. A., Eds.; John Wiley & Sons: New York, 1988; Vol. 70, Part 2, p 1.

(17) Lewis, G. J.; Hayashi, R. K.; Dahl, L. F., to be published.

(18) The naturally occurring isotopes of platinum are ^{190}Pt (0.01%), ^{192}Pt (0.79%), ^{194}Pt (32.9%), ^{195}Pt (33.8%), ^{196}Pt (25.3%), and ^{198}Pt (7.2%).

(19) Kharas, K. C. C.; Dahl, L. F., to be published.

Promotion of Electron Transfer by Protonation of Nitrogen-Centered Free Radicals. The Addition of Radicals to Iminium Ions[1]

Glen A. Russell,* Ching-Fa Yao, Ragine Rajaratnam, and Byeong Hyo Kim

Department of Chemistry, Iowa State University
Ames, Iowa 50011

Received August 3, 1990
Revised Manuscript Received October 1, 1990

Chain reactions between alkylmercury halides and some electron-deficient alkenes $[CH_2{=}CH(EWG)]$ involving eq 1 have been reported, e.g., with EWG = $PhSO_2$ or $(EtO)_2P(O)$.[2] Although α,β-unsaturated carbonyl compounds react inefficiently with RHgCl when photostimulated, reactions occur readily in the presence of iodide ion in Me_2SO by virtue of electron transfer between the adduct enolyl radical and $RHgI_2^-$, eq 2.[3,4] However, adduct radicals from α,β-unsaturated nitriles do not undergo this reaction efficiently.

$$RCH_2CH(EWG)^\bullet + RHgCl \rightarrow RCH_2CH(HgCl)EWG + R^\bullet \tag{1}$$

$$RCH_2\dot{C}HC(O)Y + RHgI_2^- \rightarrow RCH_2CH{=}C(O^-)Y + R^\bullet + HgI_2 \tag{2}$$

We have found that intermediate adduct radicals such as $RCH(R^1)\dot{C}(Y)C{\equiv}N \leftrightarrow RCH(R^1)C(Y){=}C{=}\dot{N}$ or $RCH_2\dot{C}(R^1)C(Y){=}NR^2 \leftrightarrow RCH_2C(R^1){=}C(Y)\dot{N}R^2$, although often unreactive in reaction 1 or 2, will undergo chain propagation reactions with $RHgI/I^-$ in the presence of proton donors such as *p*-toluenesulfonic acid (PTSA), eqs 3 and 4. In the absence of

---

(1) Electron Transfer Processes. 52. Supported by Grant CHE-8717871 from the National Science Foundation and by the donors of the Petroleum Research Fund, administered by the American Chemical Society.

(2) Russell, G. A.; Jiang, W.; Hu, S. S.; Khanna, R. K. *J. Org. Chem.* **1986**, *51*, 5498. Russell, G. A. *Acc. Chem. Res.* **1989**, *22*, 1.

(3) Russell, G. A.; Hu, S.; Herron, S.; Baik, W.; Ngoviwatchai, P.; Jiang, W.; Nebgen, M.; Wu, Y.-W. *J. Phys. Org. Chem.* **1988**, *1*, 299.

(4) Russell, G. A.; Baik, W.; Ngoviwatchai, P.; Kim, B. H. *Acta Chem. Scand.* **1990**, *44*, 170.

Table I. Free Radical Alkylations Utilizing t-BuHgI/KI/PTSA in Me_2SO[a]

substrate	t-BuHgI:KI:PTSA (equiv)	products (% yield)[b]	
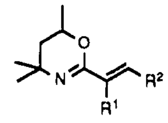		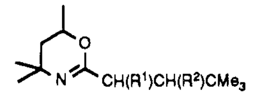	
R^1 = Ph, R^2 = H	5:5:0	not detected[c]	
R^1 = Ph, R^2 = H	5:5:3	>95	
R^1 = Me, R^2 = H	2:4:0	30[d]	
R^1 = Me, R^2 = H	5:5:3	>95	
R^1 = H, R^2 = Ph	5:5:0	no reaction	
R^1 = H, R^2 = Ph	5:5:3	65[e]	
$CH_2{=}CHCN$	1:3:0	t-$BuCH_2CH_2CN$ (<5)[f]	
$CH_2{=}CHCN$	2:4:0	t-$BuCH_2CH_2CN$ (30), [t-$BuCH_2CH(CN)-]_2$ (35)	
$CH_2{=}CHCN$	1:3:3	t-$BuCH_2CH_2CN$ (33), t-$BuCH_2CH_2CONH_2$ (24)[g]	
(E,Z)-$MeCH{=}CHCN$	2:2:0	t-$BuCH(Me)CH_2CN$ (<16)	
(E,Z)-$MeCH{=}CHCN$	2:2:3	t-$BuCH(Me)CH_2CN$ (60), t-$BuCH(Me)CH_2CONH_2$ (12)	
(E)-$NCCH{=}CHCN$	2:0:0	t-$BuCH(CN)CH_2CN$ (<2)	
(E)-$NCCH{=}CHCN$	2:2:0	t-$BuCH(CN)CH_2CN$ (44), t-$BuC(CN){=}CHCN$ (14)	
(E)-$NCCH{=}CHCN$	2:2:3	t-$BuCH(CN)CH_2CN$ (<95)	
$CH_2{=}C(Cl)CN$	5:5:0	t-$BuCH_2CH(Cl)CN$ (20)	
$CH_2{=}C(Cl)CN$	5:5:5	t-$BuCH_2CH(Cl)CN$ (65), [t-$BuCH_2C(CN){=}]_2$ (13)	
t-$BuC(CN){=}CHCN$	5:5:3	t-$BuCH(CN)CH(CN)Bu$-t (75)[h]	
$PhCH{=}C(CN)_2$	2:4:0	$PhCH(t\text{-}Bu)CH(CN)_2$ (41)	
$PhCH{=}C(CN)_2$	2:4:4	$PhCH(t\text{-}Bu)CH(CN)_2$ (91)	
$Me_2C{=}C(CN)_2$	2:2:3	t-$BuCMe_2CH(CN)_2$ (100)	
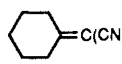	3:0:0 3:3:0 3:3:3	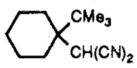	(37)[i] (68) (100)
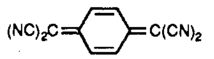	5:5:5	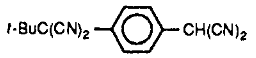	(86)

[a] Photostimulation by a 275-W fluorescent sunlamp ca. 20 cm from a Pyrex reaction tube for 23 h at 35–40 C; PTSA = p-toluenesulfonic acid. Workup with aqueous $Na_2S_2O_3$ and CH_2Cl_2 extraction after neutralization. [b] By ^1H NMR with $PhCH_3$ as an internal standard. [c] Dimer of adduct radical formed in ~40% yield. [d] Dimer of adduct radical formed in 35% yield. [e] Dimer of adduct radical formed in 15% yield. [f] Major products were [t-$BuCH_2CH(CN)-]_2$ and oligomers. [g] Dimer or oligomers not detected. [h] One-to-one mixture of diastereomers. [i] Thirty-seven percent of starting nitrile recovered.

a proton donor, dimerization products are the major products observed for vinylaminyl radicals while for t-$BuCH_2CH(CN)^•$ the proton donor decreases the yield of the dimerization or oligomerization products and increases the yield of t-$BuCH_2CH_2CN$/t-$BuCH_2CH_2CONH_2$ (Table I). The reductive alkylations summarized in Table I fail to occur in the absence of chain initiation and in most cases in the absence of I^-.[5]

$$\wr{=}C{=}NH^{•+} + RHgI_2^- \xrightarrow{Me_2SO} \wr{=}C{=}NH + R^• + HgI_2 \quad (3)$$

$$\wr{=}C(Y)NH(R^1)^{•+} + RHgI_2^- \xrightarrow{Me_2SO} \wr{=}C(Y)NH(R^1) + R^• + HgI_2 \quad (4)$$

The addition of t-$Bu^•$ to Mannich or Schiff bases ($R^1N{=}CHR^2$), or to the corresponding iminium ions, occurs exclusively at the carbon atom even when R^1 = alkyl and R^2 = aryl. The reactivities relative to (E)-$PhCH{=}CHI$ (which yields (E)-$PhCH{=}CHCMe_3$)[6] increase upon conversion of the imine to the iminium ion. Thus the relative reactivities of c-$C_6H_{11}N{=}CHPh$, $PhN{=}CHPh$, and 2,6-(i-Pr)$_2C_6H_3N{=}CH_2$ increase upon protonation by PTSA from 0.03, 0.6, and 0.6 to 13, 4, and 7, respectively. The amine radical cations [$R^1NHCH(R^2)CMe_3^{•+}$] formed from the iminium ions are readily reduced by t-BuHgCl/KI to form the amine in a chain reaction. Thus, the yields of the amines formed in 1.5 h in Me_2SO with sunlamp photolysis increased in the presence of PTSA from 0 to 88% for c-$C_6H_{11}N{=}CHPh$ and from 2 to 80% for $PhN{=}CHPh$. Similar increases in reactivity and yield were observed upon trimethylsilation of the imines by trimethylsilyl iodide (TMSI). However, the relative reactivities of α,β-unsaturated nitriles are not increased by the presence of PTSA, suggesting that for the nitriles protonation follows the addition of the *tert*-butyl radical whereas for imines protonation precedes the radical addition step.

Preformed iminium ions such as **1** (reaction 5) undergo a chain reaction with t-BuHgCl/KI upon photolysis. Since α-amino alkyl radicals are readily oxidized to iminium ions,[7] even by alkylmercury halides,[8] the chain reaction of Scheme I occurs readily.

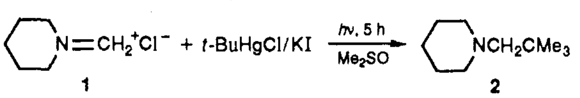

1 **2** (5)

Scheme I

$$R^1R^2NCH_2SPh + t\text{-}Bu^• \rightarrow R^1R^2NCH_2^• + t\text{-}BuSPh$$

$$R^1R^2NCH_2^• + t\text{-}BuHgX \rightarrow \mathbf{1} + t\text{-}Bu^• + Hg^0 + X^-$$

$$\mathbf{1} + t\text{-}Bu^• \rightarrow R^1R^2NCH_2CMe_3^{•+}$$

$$R^1R^2NCH_2CMe_3^{•+} + t\text{-}BuHgI_2^- \rightarrow \mathbf{2} + t\text{-}Bu^• + HgI_2$$

---

(5) Reaction of an excess of acrylonitrile with t-BuHgCl/$NaBH_4$ in CH_2Cl_2 forms t-$BuCH_2CH_2CN$ in 58% yield via the reaction of t-$BuCH_2CHCN$ with RHgH. Giese, B. *Radicals in Organic Synthesis: Formation of Carbon-Carbon Bonds*; Pergamon Press: New York, 1986; p 40. See also: Giese, B.; Meister, J. *Chem. Ber.* **1977**, *110*, 2588. In the presence of KI and PTSA in Me_2SO, a similar hydrogen atom transfer from low concentrations of HI could conceivably be involved. However, when the adduct radical does not contain an easily protonated radical center, promotion from KI/PTSA is not observed. Thus, the photochemical reaction of t-BuHgCl/KI with chalcone to form $PhCH_2CH(COPh)CMe_3$ is not promoted by PTSA, and yields of the reductive β-alkylation products of other α,β-unsaturated ketones are reduced by the presence of PTSA.

(6) Russell, G. A.; Ngoviwatchai, P.; Tashtoush, H. I.; Pla-Dalmau, A.; Khanna, R. K. *J. Am. Chem. Soc.* **1988**, *110*, 3530.

(7) Radicals of the type $R_2NCR_2^•$ are known to have low oxidation potentials with $E_{1/2}^{ox}$ in the range of -1 V (SCE). Hawari, J. A.; Knabus-Kominska, J. M.; Wayner, D. D. M.; Griller, D. *NATO ASI Ser., Ser. C* **1986**, *189*, 91. The irreversible half-wave reduction potentials of alkylmercury halides are typically more positive than -0.6 V (SCE). Kurosowa, H.; Okada, H.; Hattori, T. *Tetrahedron Lett.* **1981**, *22*, 4495.

Photolysis of $R^1R^2NCH_2SPh$ with *t*-BuHgCl/KI in Me_2SO forms **2** (65%) and *t*-BuSPh (75%) while $PhNHCH_2SPh$ yields $PhNHCH_2CMe_3$ in 61% yield. In Scheme I an organomercurial serves as both an oxidizing agent (*t*-BuHgX in step 2) and a reducing agent (*t*-$BuHgI_2^-$ in step 4). (The value of $K_{complexation}$ for *t*-BuHgI and I^- is ~1 M^{-1} in Me_2SO.[3]) The reaction fails to occur in the absence of iodide ion required for the reduction step.

---

(8) Russell, G. A.; Kulkarni, S. V.; Khanna, R. K. *J. Org. Chem.* **1990**, *55*, 1080. Adduct radicals from enamines undergo electron transfer to $PhCOCH_2HgCl$, and a similar free radical chain alkylation of enamines is observed with fluorohalocarbons (Rico, L.; Cantacuzene, D.; Wakselman, C. *Tetrahedron Lett.* **1981**, 3405) or *p*-$O_2NC_6H_4CH_2Cl$ (unpublished results with Dr. Keyang Wang). Protonation which would lead to the distonic radical cation ($>N^+H\dot{C}HR'$) does not promote the reaction of enamines with RHgX/KI.

Halogenated Peroxyl Radicals as Two-Electron-Transfer Agents. Oxidation of Organic Sulfides to Sulfoxides

Christian Schöneich, Ahmed Aced, and Klaus-Dieter Asmus*

Hahn-Meitner-Institut Berlin, Bereich S
Abteilung Strahlenchemie, Postfach 390128
1000 Berlin 39, Federal Republic of Germany

Received September 5, 1990
Revised Manuscript Received October 29, 1990

Halogenated peroxyl radicals, R(Hal)OO•, are known as efficient one-electron oxidants.[1] Rate constants for such 1e reactions generally increase with the degree of halogenation and depend on the redox potentials of the donors.[2-4] Exceptions to these trends have, however, been noted for some R(Hal)OO•-induced sulfide and selenide oxidations.[5,6] In this communication we provide evidence that R(Hal)OO• may also be involved in two-electron-transfer processes and that in the case of sulfide oxidation this is a direct route to sulfoxide.

Figure 1a shows the time-resolved conductivity change obtained upon pulse radiolysis of an aqueous, air-saturated, pH 4 solution containing 5×10^{-3} M CCl_4, 8×10^{-5} M chlorpromazine (CPZ), and 1.0 M *tert*-butyl alcohol. Dissociative electron capture by CCl_4 yields 1 equiv of H^+/Cl^- ions, evidenced by the fast increase in conductivity during the 1-μs pulse.[7] The $CCl_3OO^\bullet$ radical formed by O_2 addition to $^\bullet CCl_3$[8] oxidizes CPZ in a 1e process:[3]

$$CCl_3OO^\bullet + CPZ + H^+ \rightarrow CPZ^{\bullet+} + CCl_3OOH \tag{1}$$

The $CPZ^{\bullet+}$ is identified by its optical absorption (λ_{max} = 515 nm).[9] The associated decrease in conductivity reflects the replacement of the highly conducting protons by the less conducting $CPZ^{\bullet+}$ radical cations[10] and shows that the hydroperoxide does not decay into ionic species over the experimental time scale. Qualitatively the same (with lower rates) applies for $CHCl_2OO^\bullet$ radicals.

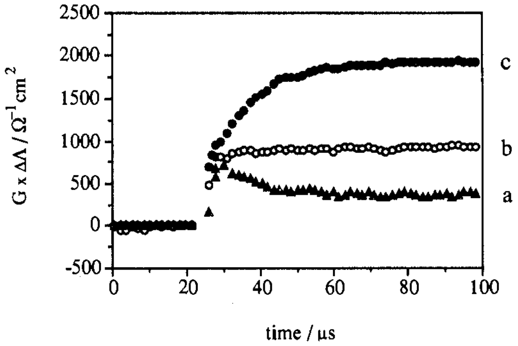

Figure 1. Conductivity (in units of $G \times \Delta\Lambda$) vs time trace obtained upon pulse radiolysis (pulse length ≈ 1 μs) of an aqueous, air-saturated, 1.0 M *tert*-butyl alcohol solution containing (a) 5×10^{-3} M CCl_4 and 8×10^{-5} M chlorpromazine (CPZ), pH 4.1; (b) 5×10^{-3} M CCl_4 and 1.0×10^{-3} M Me_2S, pH 4.0; and (c) 1×10^{-2} M $CHCl_3$ and 7.4×10^{-3} M Me_2S, pH 4.3.

One-electron oxidation of dimethyl sulfide by R(Hal)OO• leads to $(Me_2S\therefore SMe_2)^+$ radical cations (λ_{max} = 465 nm)[11] with yields of ≈75% and ≈50% for $CCl_3OO^\bullet$-induced (10^{-3} M Me_2S, $k = 1.8 \times 10^8$ M^{-1} s^{-1})[5] and $CHCl_2OO^\bullet$-induced (7.4×10^{-3} M Me_2S, 1.0×10^7 M^{-1} s^{-1}) reactions, respectively. The corresponding conductivity signals (Figure 1, parts b and c), in comparison to the CPZ system, show formation of additional yields of charged species. Thus, the net decrease caused by 1e oxidation is practically compensated in the CCl_4/Me_2S system, while in the $CHCl_3/Me_2S$ system the final conductivity (rising with the same rate as the 1e process) attains even more than twice the initial signal.

High yields of dimethyl sulfoxide are generated in our $CCl_4/CHCl_3$–O_2–Me_2S–Me_3COH systems,[12] e.g. (in terms of *G* units[13]): *G*(DMSO) = 2.1 in $CCl_4/10^{-3}$ M Me_2S, 3.55 in $CHCl_3/10^{-3}$ M Me_2S, and 5.0 in $CHCl_3/7.4 \times 10^{-3}$ M Me_2S systems. Part of it results from sulfide oxidation through $^\bullet OOCH_2CMe_2OH$ radicals and by decay of the 1e intermediate $[Me_2S\therefore SMe_2]^+$. The respective contributions are calculable on the basis of experiments on exclusive Me_2S oxidation by •OH or $^\bullet OOCH_2CMe_2OH$, respectively.[14] The remainder, which also results from R(Hal)OO• but not via the 1e mechanism, accounts for *G* = 0.45, 2.4, and 2.25 in the above three systems, respectively.

All observations concerning the sulfide oxidation are accounted for by assuming an adduct formation as the first step. The resulting sulfuranyl-type radical is likely to be polarized (I), possibly in "hydrated" form (Ia) (after inclusion of OH^- and H^+ and reversal of polarization): The addition formally constitutes a 1e oxidation of the sulfide function. A displacement reaction with a second sulfide (eq 3) receives its driving force from the stabilization of the three-electron bond.[11,15] Alternatively, an intra-

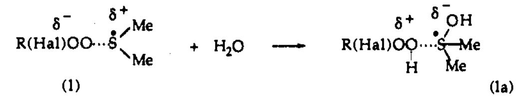

(1) (1a) (2)

$$R(Hal)OO^{\delta-}\cdots {}^{\bullet}S^{\delta+}Me_2 + H_2O \longrightarrow R(Hal)O^{\delta+}(H)O\cdots {}^{\bullet}S(OH^{\delta-})Me_2 \tag{2}$$

$$I/Ia + Me_2S \rightarrow (Me_2S\therefore SMe_2)^+ + R(Hal)OO^- (+H_2O) \tag{3}$$

---

(1) Packer, J. E.; Slater, T. F.; Willson, R. L. *Life Sci.* **1978**, *23*, 2617.

(2) Alfassi, Z. B.; Mosseri, S.; Neta, P. *J. Phys. Chem.* **1987**, *91*, 3383.

(3) Lal, M.; Schöneich, C.; Mönig, J.; Asmus, K.-D. *Int. J. Radiat. Biol.* **1988**, *54*, 773.

(4) Neta, P.; Huie, R. E.; Mosseri, S.; Shastri, L. V.; Mittal, J. P.; Maruthamuthu, P.; Steenken, S. *J. Phys. Chem.* **1989**, *93*, 4099.

(5) Mönig, J.; Göbl, M.; Asmus, K.-D. *J. Chem. Soc., Perkin Trans. 2* **1985**, 647.

(6) Schöneich, C.; Narayanaswami, V.; Asmus, K.-D.; Sies, H. *Arch. Biochem. Biophys.* **1990**, *282*, 18.

(7) Köster, R.; Asmus, K.-D. *Z. Naturforsch.* **1971**, *26b*, 1104.

(8) Mönig, J.; Bahnemann, D.; Asmus, K.-D. *Chem.-Biol. Interact.* **1983**, *47*, 15.

(9) Mönig, J.; Asmus, K.-D.; Schaeffer, M.; Slater, T. F.; Willson, R. L. *J. Chem. Soc., Perkin Trans. 2* **1983**, 1133.

(10) Asmus, K.-D.; Janata, E. In *The Study of Fast Processes and Transient Species by Electron Pulse Radiolysis*; Baxendale, J. H., Busi, F., Eds.; NATO ASI Series, Series C, 86; D. Reidel Publishing Company: Dordrecht, 1982; p 91.

(11) Göbl, M.; Bonifacic, M.; Asmus, K.-D. *J. Am. Chem. Soc.* **1984**, *106*, 5984.

(12) Analysis was performed on HPLC using an Inertsil column (250 × 4.6 mm, 5μ, ODS II) and UV detection at 210 nm. The eluent was isocratic methanol/water (5:95, v/v) at 1 mL/min. Radiation chemical conversions were generally kept to ≤10% to avoid secondary reactions to, e.g., higher oxidation states such as sulfones.

(13) *G* denotes the number of molecules generated/100 eV absorbed radiation energy. Initial R(Hal)OO• (from e_{aq}^- + halocarbon reaction) and $^\bullet OOCH_2CMe_2OH$ (from •OH + *tert*-butyl alcohol) yields are *G* = 2.8.

(14) For •OH reactions irradiations were carried out with N_2O/O_2 (4:1 v/v) saturated solutions, 1×10^{-3} M Me_2S, pH 6; for $^\bullet OOCH_2CMe_2OH$ reactions solutions were air-saturated and contained 1 M *tert*-butyl alcohol in addition to Me_2S. DMSO formation from $^\bullet OOCH_2CMe_2OH$ seems to occur only via the 2e process.

0002-7863/91/1513-375$02.50/0